

Obtaining transverse cooling with nonmagnetized electron beam

S. Seletskiy^{✉,*}, M. Blaskiewicz, A. Drees[✉], A. Fedotov, W. Fischer[✉], X. Gu, R. Hulsart, D. Kayran, J. Kewisch, C. Liu, M. Minty[✉], V. Ptitsyn, V. Schoefer, A. Sukhanov, P. Thieberger[✉], and H. Zhao

Brookhaven National Laboratory, Upton, New York 11973, USA



(Received 24 July 2020; accepted 16 November 2020; published 30 November 2020)

The first electron cooling with rf-accelerated electron bunches was recently demonstrated at the low energy RHIC electron cooler (LEReC) at BNL. Successful cooling requires that the electrons in the cooling section have a small angular spread and are well aligned with respect to the copropagating ions. LEReC puts into practice a nonmagnetized cooling of the ions at Lorentz factors of $\gamma = 4.1$ and 4.9 . Hence, unlike in previous coolers, in which the transverse electron dynamics is constrained by longitudinal solenoid fields, the ion-electron focusing and steering strongly contribute to the average angular spread of the electron beam. In this paper we discuss the factors that affect the electron angles and describe the process of tuning the electron beam to maximize the cooling of ion bunches in RHIC.

DOI: [10.1103/PhysRevAccelBeams.23.110101](https://doi.org/10.1103/PhysRevAccelBeams.23.110101)

I. INTRODUCTION

Two operational methods of increasing the phase space density of ion bunches in the collider are electron cooling [1] and stochastic cooling [2]. Stochastic cooling was implemented at the Relativistic Heavy Ion Collider (RHIC) [3] in 2008. The world's first electron cooling of colliding ion bunches was successfully demonstrated at RHIC in 2019 [4].

Electron cooling increases the phase space density of bunches of heavy particles through their interaction with copropagating bunches of “cold” electrons, which introduce dynamical friction [5].

Electron Cooling, invented by Budker in 1967 and demonstrated in 1974 [6], was implemented at numerous nonrelativistic (with Lorentz $\gamma \lesssim 1.5$) proton and ion storage-rings [7]. The first relativistic electron cooling was demonstrated at Fermilab in 2005 [8,9].

In a typical electron cooler a DC electron beam is generated from a thermionic cathode immersed in a solenoidal magnetic field [10]. The cooling section (CS) of a typical cooler, a straight section of the storage ring where electrons copropagate with ions at the same average velocity, is immersed in a continuous solenoidal field matching [11] the field at the cathode. After each passage the electrons are either dumped or returned to the gun for

charge recovery, thus, on each turn the ions interact with fresh electrons. Over many revolutions in the accelerator the average friction reduces both the transverse and the longitudinal momentum spread of the ion bunch. Experiments with electron pulses in conventional coolers were performed at IMP [12,13].

Unlike previous coolers, which utilize magnetized DC electron beam, LEReC features electron bunches produced from a photo-cathode and accelerated in rf cavities. The LEReC electron beam is “nonmagnetized,” that is neither the gun nor the cooling section are immersed in the solenoidal field. Due to these design aspects, the LEReC beam dynamics differs significantly from dynamics in previous electron coolers.

The velocity distribution in the electron bunches suitable for rf acceleration is close to be spherically symmetric, while in both the DC beams and in the electrostatically accelerated long pulses of electrons the velocity distribution is “flat”—with longitudinal velocity spread being orders of magnitude smaller than the transverse velocity spread. As a result, in DC coolers the longitudinal cooling is much stronger than the transverse one. In LEReC, on the other hand, by design both the longitudinal and the transverse cooling rates are the same.

In the DC coolers the strong continuous solenoidal field along the CS and the electron beam magnetization on the cathode “freeze” the transverse beam dynamics in the cooling section. The effective transverse cooling is achieved as long as the CS solenoid is aligned with the trajectory of the cooled ions through the CS. LEReC is the first cooler using non-magnetized electron beam. Hence, various beam dynamics considerations not relevant for previous coolers are essential for achieving the good

*seletskiy@bnl.gov

Published by the American Physical Society under the terms of the Creative Commons Attribution 4.0 International license. Further distribution of this work must maintain attribution to the author(s) and the published article's title, journal citation, and DOI.

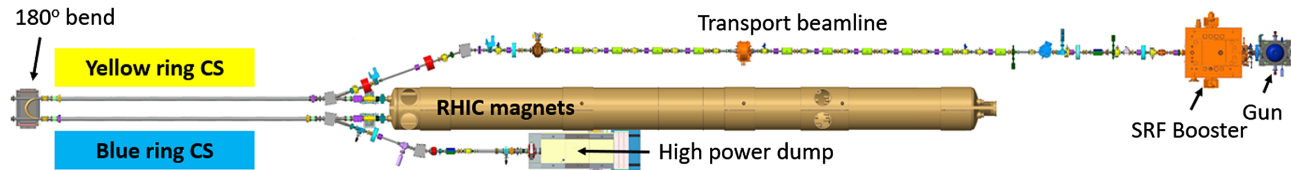


FIG. 1. Schematics of LEReC layout (not to scale).

transverse cooling rate in LEReC. An electron beam emittance, an ion-electron focusing and an ion-electron trajectory kick, as well as specific measures to keep the cooling section free from magnetic field are the important aspects unique to the LEReC approach to cooling.

For medium energy relativistic electron coolers the LEReC approach significantly simplifies the engineering design. Even more importantly, because of technical difficulties associated with electrostatic acceleration of the DC electron beam to high energies, an rf acceleration and bunched electron beam is the most feasible approach for electron cooling in future colliders [14]. For example, a number of effects studied in the LEReC and discussed in this paper are shaping currently conducted feasibility studies of an electron cooler for the Electron Ion Collider [15], which will be built at BNL.

In this paper after a short introduction to LEReC we derive the dependence of the transverse cooling force on relative electron-ion angles (Sec. II). Next, in Sec. III, we discuss various factors affecting both the angular spread of the electron bunches and the misalignment of electron and ion trajectories in the CS. We describe the measures for mitigating the effects causing the growth of electron angles, essentially providing a recipe for building a functional non-magnetized electron cooler. Finally, in Sec. IV, we discuss our experience with achieving the world’s first transverse electron cooling with non-magnetized rf-accelerated electron bunches.

LEReC is an integral part of RHIC operation dedicated to the search for a critical point in the phase diagram of nuclear matter. LEReC was built to counteract the intra-beam scattering (IBS) in the ion bunches with relativistic factors $\gamma = 4.1$ and 4.9 , which correspond to electron beam kinetic energies of 1.6 MeV and 2 MeV.

The LEReC layout is schematically shown in Fig. 1.

The LEReC photo-cathode is illuminated by a green 704 MHz laser modulated with the 9 MHz frequency to match the frequency of RHIC ions. The resulting 9 MHz “macro bunches” of electrons consist of thirty 704 MHz bunches each. When overlapped with the ion bunch in the cooling section the electron macro-bunch covers $\pm 2\sigma$ of longitudinal span of the ion bunch (see Fig. 2). Where σ is the root mean square (rms) length of the ion bunch, which has a Gaussian longitudinal distribution.

The electrons are accelerated nominally to 400 keV in the dc gun [16] followed by a 704 MHz superconducting rf

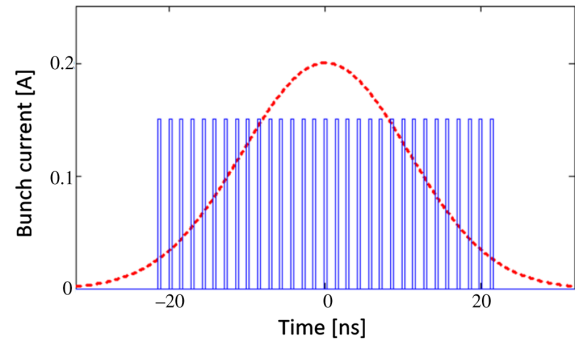


FIG. 2. Longitudinal distribution of the ion bunch (dashed red line) overlapped with the electron macro-bunch (solid blue line) containing thirty bunches.

accelerating cavity (SRF Booster) [17] bringing the beam energy to 1.6 – 2 MeV.

The electron beam is transported in a 40 m long transport beamline and merged to the cooling section in the “Yellow” RHIC ring via a dispersion-free merger dogleg. After passing the Yellow CS, the beam is sent to the cooling section in the “Blue” RHIC ring by a 180° bend. Thus, the same electron bunches are utilized to cool the ions in both rings of the collider—another unique feature of LEReC. The electron beam is extracted at the exit of the blue CS through the extraction dogleg and sent to the beam dump. The focusing throughout LEReC is intermittent and provided by the solenoids. A few matching quadrupoles that preserve the rotational symmetry of the electron beam are located near the bending magnets (marked gray in Fig. 1). More details of the LEReC setup can be found in [4,16,18–20].

Both the Yellow and the Blue cooling sections are 20 m long. Each LEReC CS contains 8 short solenoids combined with dipole correctors and beam position monitors (BPMs) located downstream of each solenoid. The distance between solenoid centers (L_{s2s}) is 3 m. The cooling sections are schematically shown in Fig. 3.

The solenoids in LEReC CS, which are used for correction of the beam envelope, occupy less than 10% of its length. Since the electron beam is non-magnetized the effective cooling takes place only in the regions free from the longitudinal magnetic field. Therefore, special measures (discussed in Sec. III B) must be taken to minimize the expanse of the solenoidal field into the drifts between the solenoids.

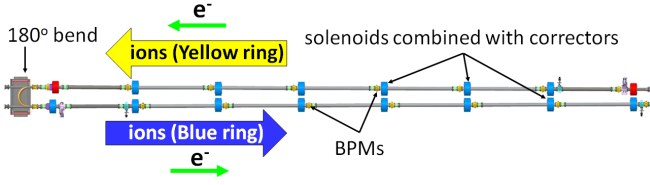


FIG. 3. The layout of the LEReC cooling sections.

II. ELECTRON BEAM REQUIREMENTS IN THE COOLING SECTIONS

The friction force acting on the ion due to its interaction with a nonmagnetized electron bunch with velocity distribution $f(v_e)$ is given by [21,22]:

$$\vec{F} = -\frac{4\pi n_e e^4 Z^2}{m_e} \int L_C \frac{\vec{v}_i - \vec{v}_e}{|\vec{v}_i - \vec{v}_e|^3} f(v_e) d^3 v_e. \quad (1)$$

Here, n_e is the electron bunch density in the beam frame, e is the electron charge, $Z \cdot e$ is the ion charge, m_e is the mass of the electron, \vec{v}_i and \vec{v}_e are ion and electron velocities in the beam frame. The Coulomb logarithm is $L_C = \ln(\rho_{\max}/\rho_{\min})$ with a minimal impact parameter $\rho_{\min} = (Ze^2)/(m_e |\vec{v}_i - \vec{v}_e|^2)$. A maximum impact parameter ρ_{\max} is determined by the time of flight of the ions through the CS. The Coulomb logarithm can be assumed to be constant, in the LEReC case $L_C \approx 8$. We assume a Gaussian distribution of velocities in the electron bunch with rms values Δ_t and Δ_z for transverse and longitudinal velocity components respectively.

LEReC was designed to cool ion bunches with an expected rms longitudinal and transverse velocity spread (in the beam frame) of 1.5×10^5 m/s and 1.7×10^5 m/s respectively.

Integration of Eq. (1) shows that the friction force is linear for the longitudinal ion velocity $v_{iz} \lesssim \Delta_z$ [18]. Since the cooling under discussion is directly applied to the ions in the collider, it is important not to overcool the ion bunch. Therefore, the requirement for the rms spread of the electron bunch longitudinal velocities is $\Delta_z \approx 1.5 \times 10^5$ m/s. From similar considerations follows $\Delta_t \approx 1.7 \times 10^5$ m/s. Converting the longitudinal and transverse velocity spreads in the beam frame into relative energy spread (σ_δ) and angular spread (σ_θ) in the laboratory frame respectively, we obtain the following requirements for the LEReC electron bunch parameters:

$$\sigma_\delta = \frac{\Delta_z}{\beta c} = 5 \times 10^{-4}; \quad \sigma_\theta = \frac{\Delta_t}{\gamma \beta c} = 150 \mu\text{rad}. \quad (2)$$

The average velocity of the two beams must be matched to better than the rms velocity spread. Therefore, equations (2) set the respective requirements for the matching of the relativistic γ -factors of ion and electron beams [18] and for the alignment of the electron and ion trajectories in the

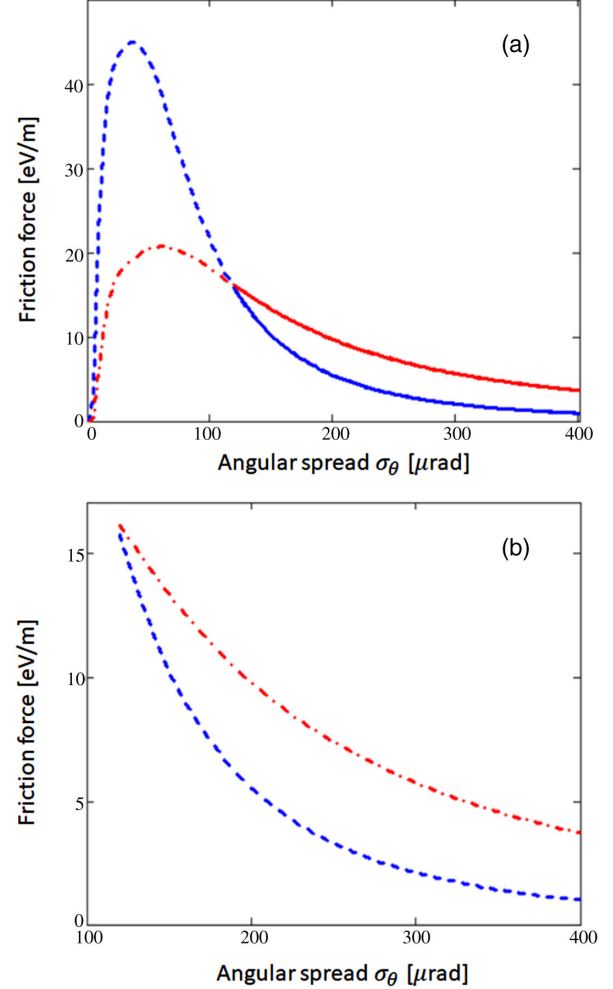


FIG. 4. Transverse (blue dash line) and longitudinal (red dot-dash line) friction force depending on the rms angular spread of the electron bunch. The solid lines in the plot (a) show the friction force for the range of realistically achievable electron angles. The plot (b) is a zoomed-in view of the realistic parameters range. The force is calculated for an ion with $v_i = \sqrt{v_i^2}$ and for beam parameters from the experiment described in Section IV by integrating Eq. (1) over the electron bunch velocity distribution.

CSs. Producing the electron bunches with satisfactory energy spread and matching the electron and ion γ -factors was enough to demonstrate the first rf-based cooling [18]. Yet, optimizing the cooling, especially the cooling of the transverse phase space, and increasing the RHIC luminosity required an elaborate work on electron beam focusing and trajectory in the cooling sections.

As Fig. 4 shows, for the realistically achievable LEReC parameters, the transverse component of the cooling force has a much stronger dependence on the electron angles than the longitudinal component. For example, when the transverse angular spread is increased by a factor of two from its design value, the longitudinal cooling force is reduced by about 50% while the transverse cooling force drops by more than a factor of four.

III. VARIOUS FACTORS AFFECTING ELECTRON ANGLES

A. Beam emittance

The LEReC bunches in the cooling section are required to have the transverse normalized rms emittance of $\varepsilon < 2.5 \mu\text{m}$ [4].

Because of low rigidity of the electrons the dynamics of the electron bunches is dominated by space charge effects [23].

The active area of the LEReC photo-cathode is illuminated by a 4 mm diameter laser spot with a pseudo flat-top transverse distribution obtained by removing the tails of the Gaussian laser pulse. The two short solenoids located between the gun exit and the SRF booster are used to focus the beam into the booster cavity, thus minimizing the projected bunch emittance.

The long transport line following the booster also serves as a bunch stretcher. It uses the energy chirp implemented in the booster and the ballistic stretching to increase the rms length of the bunch from about 80 ps out of the booster to about 400 ps at the CS entrance, reducing the bunch space charge significantly. For operational LEReC parameters, the peak current after ballistic stretching is about 0.15 A. The space charge effect is further reduced by the smooth focusing through the transport beam line which keeps the rms transverse beam size at about 4 mm.

Detailed simulations [23] showed that the described optics provides the electron bunches needed to satisfy the LEReC requirements.

The emittance in the cooling sections was measured with the moving slits [19]. It was found that for the operational LEReC settings the normalized transverse rms emittances in both cooling sections are lower than $1.6 \text{ mm} \cdot \text{mrad}$.

B. Canonical angular momentum

The LEReC is a nonmagnetized electron cooler. The short solenoids in the LEReC cooling sections are used only to confine the beam envelope. As a result, we had to take special measures to control the longitudinal magnetic field (B_z) outside of the CS solenoidal modules.

According to Busch's theorem for axially symmetric optics the canonical angular momentum (CAM) is conserved along any of the electron trajectories [11]:

$$M_\phi = \gamma\beta m_e c r^2 \phi' - \frac{e\Phi(r)}{2\pi} = \text{const.} \quad (3)$$

Here, r , ϕ and z are the cylindrical coordinates and $\Phi = 2\pi \int_0^r B_z(\rho) \rho d\rho$ is the magnetic flux through a circle of radius r , where r is the displacement of the electron from the beam center.

For each electron, CAM is determined by its initial value on the cathode, which is zero for the LEReC case. Then, assuming that the solenoidal field is uniform over the beam

cross section we obtain from Eq. (3) the following condition on critical B_z in the CS:

$$B_z \leq \frac{2\theta_{\text{CAM}} B\rho}{\sigma_r} \quad (4)$$

where the rms beam radius in the CS $\sigma_r \approx 5.7 \text{ mm}$ and $B\rho = \frac{\gamma m_e c}{e}$ is the beam magnetic rigidity, which is equal to $6.8 \times 10^{-3} \text{ T} \cdot \text{m}$ at the LEReC lowest operational energy. Assuming that CAM-driven angles θ_{CAM} are allowed to be only one third of the total angular spread (2), we obtain from (4) that the critical longitudinal field for the drift regions of the CS is $B_z = 10^{-4} \text{ T}$.

To minimize the extent of the longitudinal field, each CS solenoid is equipped with two (the front and the back) short bucking coils creating the solenoidal field in the direction opposite to the field of the main solenoid. As a result, the solenoidal field exceeding the critical value of 10^{-4} T is contained within 30 cm of every three meters of the cooling section.

C. Ion-electron focusing

The focusing of electrons by the space charge of the ions is an important and hard to control source of the additional angular spread within the electron bunches.

This strong hadron-electron focusing (HEF) [24] cannot be canceled out by magnetic lenses. The only option for complete suppression of HEF-driven angles is to utilize weak magnetization of the electron beam together with continuous solenoidal field in the CS [8,9]. Since LEReC uses a nonmagnetized electron beam, careful optimization of electron and ion beam parameters must be performed to minimize the HEF-driven angular spread in the cooling section.

Different electron bunches within the macrobunch are focused differently. The focusing experienced by a particular electron bunch depends on its position along the ion bunch (see Fig. 2).

Note that due to limited lifetime of RHIC ions in low energy operations the intensity of the ions, and therefore the ion-electron focusing, drops by a factor of two during the RHIC store. Hence, the beam optics optimized for, for example, the beginning of a RHIC store will not be optimal in the middle of the store.

To estimate the effect of HEF on the angular spread of electrons we consider an electron bunch cotraveling with a particular longitudinal slice of the ion bunch. The electron bunches in the cooling section are well approximated by a bunch with Gaussian transverse and uniform longitudinal distributions. The longitudinal slices of the ion bunch probed by each electron bunch are short enough to be considered having a uniform longitudinal distribution.

Under an assumption of laminar motion we derive [24] an equation describing the dynamics of an individual “ r -layer” of an electron bunch in the CS (where r is the

radial displacement from the common center of both beams):

$$r'' = \frac{K_e}{r} \left[\left(1 - e^{-\frac{r_0^2}{2\sigma_{e0}^2}}\right) - \frac{I_i}{I_e} \left(1 - e^{-\frac{r^2}{2\sigma_i^2}}\right) \right] - \kappa r + \frac{\epsilon^2 r_0^4}{\sigma_{e0}^4} \cdot \frac{1}{r^3} \quad (5)$$

Here $r' = dr/ds$, s is a path length through the cooling section, $K_e = 2I_e/(I_A\beta^3\gamma^3)$, Alfvén current $I_A = 4\pi\epsilon_0 mc^3/e$, I_e is the electron bunch current, I_i is the current of the longitudinal slice of the ion bunch probed by the electron bunch, r_0 and σ_{e0} are the initial radius of the considered electron “layer” and the rms transverse size of the electron beam at the entrance of the cooling section, σ_i is the rms transverse size of the ion bunch, $\kappa = B_z^2/(2B\rho)^2$ inside the solenoids and $\kappa = 0$ in the CS drifts.

A detailed discussion of the applicability of Eq. (5) to simulations of HEF in the LEReC CS is given in [24]. In short, we integrate Eq. (5) numerically with an explicit, exactly symplectic, second order method [25]. We treat the

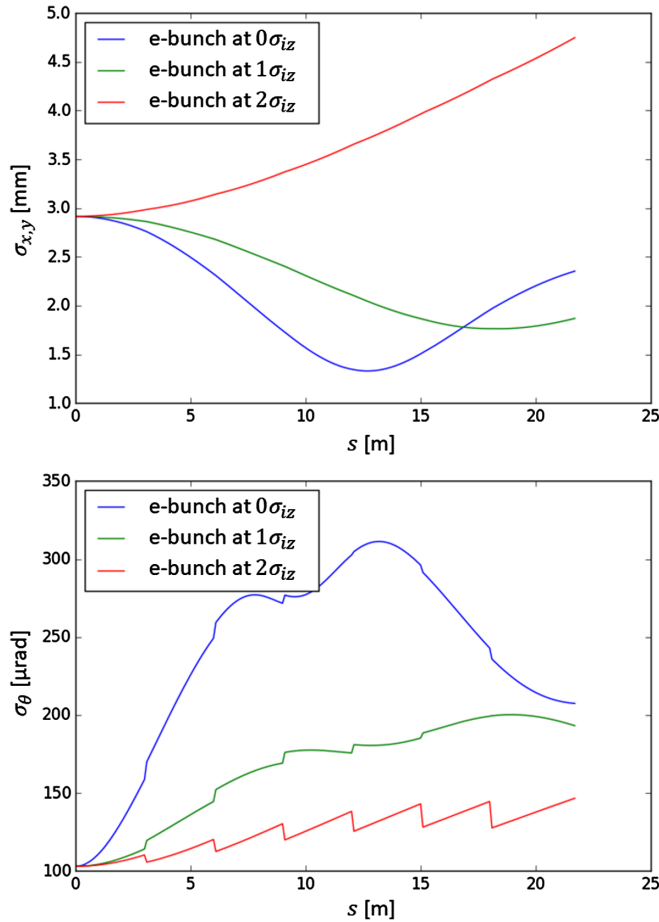


FIG. 5. RMS size (top) and rms angular spread of the electron bunches longitudinally placed at $0\sigma_{iz}$ (blue), $1\sigma_{iz}$ (green) and $2\sigma_{iz}$ (red) of the ion bunch. The results are shown for the experimental parameters listed in Table I.

CS solenoids as instantaneous focusing kicks. We benchmark the simulations for various electron beam parameters by comparing the predicted transverse distribution of the electron macrobunch focused by the ion bunch with the experimentally measured distribution. The simulated and the measured transverse distribution of the electron bunches subject to ion-electron focusing agree with an error smaller than 3%, where the discrepancy between the measured ($\mathcal{P}_{\text{meas}}$) and the simulated (\mathcal{P}_{sim}) bunch profile projections on axis x is defined as $\sqrt{\int \mathcal{P}_{\text{meas}}(\mathcal{P}_{\text{meas}} - \mathcal{P}_{\text{sim}})^2 dx} / \int \mathcal{P}_{\text{meas}} dx$. Benchmarking examples are given in [20].

The described simulations (exemplified in Fig. 5) were used to minimize the average angular spread of the electron beam. In Sec. IV we will discuss the achieved angular spread and its effect on the measured cooling rate.

D. Ion-electron trajectory kick

Another important source of potential additional angles in the cooling section is the coherent ion-electron kick [26] caused by an electron beam trajectory not being ideally aligned with the ion beam trajectory.

If the center of mass (CM) of the electron bunch is transversely displaced by d with respect to the ions CM, then from considerations similar to ones in Sec. III C:

$$d'' = -\frac{2I_i}{I_A(\beta\gamma)^3} \frac{1 - e^{-\frac{d^2}{2\sigma_i^2}}}{d} - \kappa d. \quad (6)$$

Assuming that the displacement is small in comparison to the transverse size of the ion bunch and replacing the lumped focusing in the LEReC CS with the continuous average focusing force $\bar{\kappa} = \kappa \cdot L_s/L_{s2s}$, we obtain a simple harmonic oscillator equation:

$$d'' = -d \left(\frac{I_i}{I_A(\beta\gamma)^3 \sigma_i^2} + \bar{\kappa} \right). \quad (7)$$

Solving Eq. (7) for the e-bunch trajectory angle due to the beam-beam kick $\theta_{\text{BBK}} = d'$ and requesting that $\theta_{\text{BBK}} \leq 30 \mu\text{rad}$ at any location in the CS we get the following requirement for the electron-ion displacement:

$$d \leq \frac{\sigma_i(\beta\gamma)^{3/2}}{\sqrt{I_i/I_A + \bar{\kappa}(\beta\gamma)^3 \sigma_i^2}} \theta_{\text{BBK}} = 0.22 \text{ mm}. \quad (8)$$

Simulations performed for the operational LEReC CS setup [26] confirmed requirement (8).

E. Effect of ambient field on trajectory

Ambient magnetic field is another important factor affecting the electron beam trajectory angle in the LEReC CS.

The typical ambient field mapped along the LEReC CS [27] was on the level of $30 \mu\text{T}$ with the maximum field of $50 \mu\text{T}$. On the other hand, the requirement to keep the trajectory angle due to an ambient field below $\theta_{\text{AF}} = 50 \mu\text{rad}$ results in the following requirement on the transverse magnetic field in the CS drifts:

$$B_T < \frac{B\rho\theta_{\text{AF}}}{L_{s2s}} \approx 100 \text{ nT}. \quad (9)$$

To suppress the ambient magnetic field to a tolerable level we designed and implemented a magnetic shielding for the cooling section. The typical solenoid-to-solenoid drift in the CS is shielded by two cylindrical layers of $h = 1 \text{ mm}$ thick mu-metal with magnetic permeability of $\mu = 11000$.

The shielding provided an attenuation factor of about 1000 in both horizontal and vertical directions [28] and suppressed the magnetic field in the CS below the threshold (9). This allowed us to treat the solenoid to solenoid regions as true drifts, for the purpose of electron trajectory alignment.

F. Trajectory alignment and BPMs' accuracy

The heavy ions beam trajectory through the LEReC CS is a straight line because of the ions high magnetic rigidity. Therefore, the relative alignment of the electron and ion trajectories involves two general steps.

First, one has to align the CS BPMs to the ion trajectory.

Second, one has to “zero” the electron trajectory displacement in each CS BPM by applying proper transverse kicks in the CS correctors. As discussed in Sec. III E, for a properly shielded cooling section, this step guarantees tolerable trajectory angles in the solenoid-to-solenoid drifts.

Let us assume the rms error in BPM alignment (σ_{BPM}) and error in electron trajectory alignment σ_{traj} to be equal to each other and equal to $100 \mu\text{m}$. Then for the resulting average angular error of the electron-ion trajectory alignment we obtain

$$\theta_{\text{traj}} = \frac{\sqrt{2\sigma_{\text{BPM}}^2 + 2\sigma_{\text{traj}}^2}}{L_{s2s}} \approx 70 \mu\text{rad} \quad (10)$$

which is a tolerable contribution to the total angular spread.

It is worth noting that $\sqrt{2\sigma_{\text{BPM}}^2 + 2\sigma_{\text{traj}}^2} = 200 \mu\text{m}$ also satisfies condition (8), thus guaranteeing small θ_{BCK} .

As discussed above, the CW electron beam contains both 9 MHz frequency (macrobunches) and 704 MHz frequency (repetition rate of electron bunches within one macrobunch). The ion beam spectrum is dominated by a 9 MHz frequency with much weaker higher harmonics. Each of the LEReC CS BPMs is connected to the two different processing modules, with 9 MHz and with 704 MHz signal

filtering. The procedure of the CS BPMs alignment [29] is as follows.

First, we set the desired ion trajectory through the cooling section and measure the positions of the ions in the CS BPMs (BPM_{9i0}) with 9 MHz modules.

Next, we dump the ions, send the CW electron beam through the CS and measure the electron beam positions in the CS BPMs (BPM_{9e0}) using the same 9 MHz modules.

Finally, we measure the same electron beam positions in the CS BPMs (BPM_{704e0}) with the 704 MHz modules. The ion and electron beam trajectories are aligned when $\text{BPM}_{9e0} = \text{BPM}_{9i0}$. Then, the optimal electron beam position measured with 704 MHz modules is

$$\text{BPM}_{704e} = \text{BPM}_{704e0} + (\text{BPM}_{9i0} - \text{BPM}_{9e0}) \quad (11)$$

Equation (11) gives a total (a combination of mechanical and electric) offset for each CS BPM. Automatically subtracting measured BPM_{704e} from BPMs readings we guarantee that “zeroing” of the electron beam trajectory results in successful ion-electron trajectories alignment.

The electric offset of the BPM is caused by an imbalance in scaling factors of the two channels connecting opposite BPM buttons to the processing module. If this imbalance stayed constant then the resulting error would be calibrated out by our alignment procedure once and for all. Yet, we learned from experience that there is a substantial drift of scaling factors of the BPM channels with time.

To mitigate the drift of the BPM offsets we installed switching modules [30] right next to the BPMs in the RHIC tunnel. These modules switch the signals from opposing BPM buttons between the respective channels with 760 Hz frequency, which corresponds to 1 switch per 100 revolutions of ion beam in the RHIC ring.

Let's assume that the signals induced on the two opposing BPM buttons by a passing bunch of charged particles have amplitudes A and B . The true beam position in the BPM is given by:

$$x_{\text{true}} = \zeta \frac{A - B}{A + B}. \quad (12)$$

Here ζ is the scaling coefficient and without the loss of generality we assume that there is no mechanical displacement of the BPM. Next, we assume that the signals are transferred from the BPM buttons to the processing module via the channels having different amplification (or attenuation) factors χ_1 and χ_2 . For a bunch positioned close to the BPM center, denoting $\chi_1 - \chi_2 \equiv d\chi$ and assuming $d\chi \ll \chi_1 \approx \chi_2 \equiv \chi$, we obtain the following expressions for the measurement error in the absence (x_{err1}) and in the presence (x_{err2}) of channel switching [31]:

$$x_{\text{err}1} = \zeta \frac{d\chi}{2\chi}; \quad x_{\text{err}2} = x_{\text{true}} \left(\frac{d\chi}{2\chi} \right)^2. \quad (13)$$

Equations (13) show that the BPM switching both zeroes the measurement error when the beam trajectory is centered in the BPM, and reduces the measurement error more for the better balanced channels as compared to the no-switching case.

The implementation of continuous switching of BPM channels allowed us to achieve the required accuracy of the BPM readings [31].

There is additional noise on position readings introduced by switching itself. Yet, operational parameters of the switching system were optimized to keep it on a level of a few μm (see [31] for more details).

The second step of ion-electron trajectories alignment is the correction of the electron beam trajectory. For operations an automated trajectory correction algorithm is needed.

The CS transverse correctors are overlapped with the CS solenoids to minimize the length of not-shielded regions in the CS. If a pair of transverse correctors producing horizontal (B_x) and vertical (B_y) dipole fields is immersed in a solenoid with a field B_z , then the effect of this combined magnet on the beam trajectory $\vec{X} = (x, x', y, y')^T$ is given by:

$$\vec{X}_{\text{out}} = M_s \vec{X}_{\text{out}} + \vec{V}_c \quad (14)$$

where \vec{X}_{in} and \vec{X}_{out} are the trajectory vectors at the entrance and the exit of the solenoid-corrector module, M_s is a standard solenoid matrix and \vec{V}_c represents the effect of the correctors on beam trajectory and is given by [9]:

$$\vec{V}_c = \begin{pmatrix} \frac{B_y(\cos(kL)-1)+B_x(kL-\sin(kL))}{B_z k} \\ \frac{B_x(1-\cos(kL))-B_y(kL+\sin(kL))}{2B_z} \\ \frac{B_x(1-\cos(kL))+B_y(kL-\sin(kL))}{B_z k} \\ \frac{B_y(1-\cos(kL))+B_x(kL+\sin(kL))}{2B_z} \end{pmatrix} \quad (15)$$

where $k = B_z/B\rho$ and the length L of both the solenoid and correctors is assumed to be the same.

Let us assume that the CS BPM number j measures horizontal and vertical trajectory displacements x_j and y_j respectively. Suppose there are n correctors upstream of this BPM, which are used in the trajectory correction routine. We denote the respective vectors produced by the initial settings of these correctors as \vec{V}_{0i} , where $i = 1..n$. Then the new settings of these correctors (with corresponding vectors \vec{V}_{1i}), which zero the trajectory in BPM number m , must satisfy:

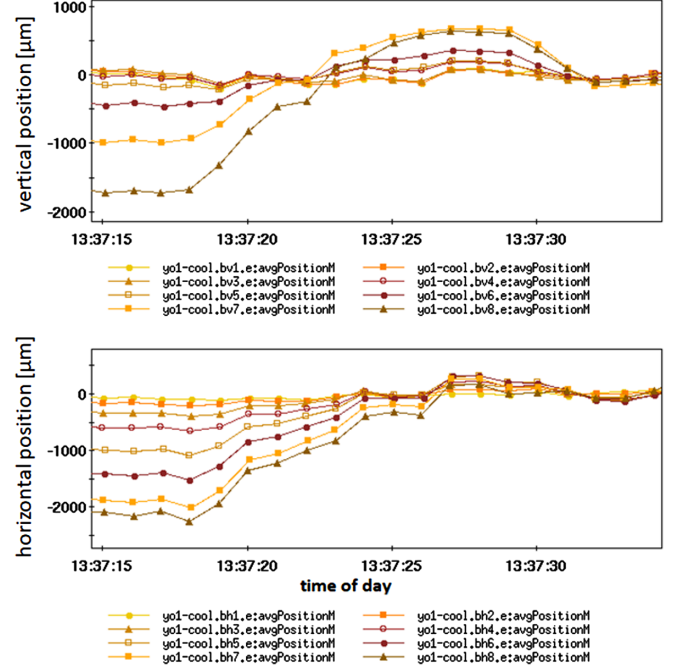


FIG. 6. Horizontal (bottom plot) and vertical (top plot) position of the electron beam measured by BPMs along the Yellow CS during application of the trajectory correction algorithm.

$$\begin{aligned} -x_j &= \sum_{i=0}^n M_{\text{tr}_{ij}}^{(1)} \cdot (\vec{V}_{1i} - \vec{V}_{0i}) \\ -y_j &= \sum_{i=0}^n M_{\text{tr}_{ij}}^{(3)} \cdot (\vec{V}_{1i} - \vec{V}_{0i}) \end{aligned} \quad (16)$$

where $M_{\text{tr}_{ij}}^{(1)}$ and $M_{\text{tr}_{ij}}^{(3)}$ are respectively the first and the third rows of the transfer matrix $M_{\text{tr}_{ij}}$ from the exit of corrector number i to the location of BPM number j .

For all m BPMs in the cooling section ($j = 1..m$), substituting Eq. (15) into Eq. (16) we get a system of $2m$ linear equations with $2N$ variables, namely, the target horizontal and vertical fields (B_{x1i} and B_{y1i} , $i = 1..N$) of N correctors utilized in the trajectory correction routine. Such a system can be easily solved in a least square sense to obtain the optimal correctors settings.

The described algorithm was implemented in the LEReC control system as a high level application written in Python. It runs on live one second averaged BPM data and it controls the correctors through RHIC HTTP service interface [32]. Its application during the cooled RHIC store is demonstrated in Fig. 6. It takes 3 iterations and about 15 seconds to correct the electron trajectory.

IV. COOLING OPTIMIZATION AND IMPROVEMENT OF RHIC LUMINOSITY

The first cooling in LEReC was observed after accurate matching of the electron and ion beam γ -factors was

achieved [18]. The obtained longitudinal cooling rate was high enough to overcome the longitudinal IBS and to provide a substantial reduction in amplitudes of synchrotron oscillations. The transverse cooling rate, on the other hand, was just enough to counteract the IBS-driven beam heating. Further improvements in transverse cooling required smaller electron-ion angles, which affect the transverse friction force much more than the longitudinal one, as discussed in Sec. II.

Numerous measurements of the electron bunch emittance in the cooling sections consistently showed that the expected electrons' thermal angular spread was about $100 \mu\text{rad}$.

The CAM-driven angular spread in the CS is basically nonexistent, since longitudinal magnetic field in the shielded CS drifts is on the scale of a few hundred nT, which is orders of magnitude smaller than the critical value (4).

The electron beam trajectory angles due to ambient fields are also negligibly small.

It was quickly realized that the two main factors contributing to the high angular spread are the ion-electron focusing and trajectory misalignment caused by drifts in scaling factors of BPM channels.

Our initial plan for mitigation of the ion-electron focusing was to run LEReC with electron bunches with a current close to or higher than the ion peak current. Such a setup would greatly reduce the space charge focusing from the ions. All thirty electron bunches in the macrobunch would actually experience some defocusing, which could be on average compensated by the CS solenoids. The high bunch charge would also provide a substantial operational safety margin in the cooling rate, which would more than compensate the partial loss in cooling because of not-ideal defocusing compensation.

These plans could not be realized because of the strong electron-ion heating [20,33], which significantly limits the available operational range of bunch charges.

The heating is a combined effect of a picket-fence temporal structure of the electron macrobunch and the synchrotron motion of an individual ion, which results in randomization of the space charge kick from electron bunch on the ion. The heating rate is proportional to the square of the strength of the kick. Hence, the heating rate grows as the square of the electron bunch density while the cooling rate is linearly proportional to the density of the bunch. As a result, we had to operate with the bunch charges of $\approx 60\text{--}70 \text{ pC}$, instead of the initially planned $100\text{--}130 \text{ pC}$.

We performed experimental optimization of such LEReC settings as the CS solenoid currents and electron beam Twiss parameters at the CS entrance using as a guide simulations described in Sec. III C. We estimate that the total angular spread (including both the thermal angles and

the HEF) averaged over 30 electron bunches and over the cooling section length is about $160 \mu\text{rad}$.

We plan to further mitigate the ion-electron focusing by two measures.

One possibility is to create a longitudinally hollow electron macrobunch. Omitting several electron bunches in the middle of the ion bunch should not affect the cooling much. These bunches are severely overfocused (see Fig. 5) with the angular spread too large to provide substantial transverse cooling. On the other hand, reduction in number of electron bunches in a macrobunch must reduce the heating effect, which will allow us to increase the charge per bunch.

Another planned measure is to upgrade the LEReC rf system to produce longer electron bunches while still keeping a small energy spread. This will allow us to increase the bunch charge while keeping the charge density, and thus the heating rate, constant. The cooling rate from the elongated electron bunches will get higher because of the increase in an effective cooling duty factor.

Both of these improvements are a subject of the planned LEReC upgrade.

The main focus of our most recent efforts to increase the transverse cooling rate was on electron-ion trajectory alignment.

It became clear that the BPM offsets, as defined in Sec. III F, drift with time. This effect was resulting in substantial trajectory misalignment and high coherent angles (both θ_{traj} and θ_{BBK}).

Implementation of continuous switching of BPM channels was a real game changer. After the switching modules were utilized and the BPM alignment procedure was reapplied, exercising the trajectory correction routine consistently resulted in good transverse cooling.

For illustration we compare two consecutive stores, one with and one without cooling.

Figure 7 shows the evolution of the rms transverse beam sizes of the colliding ions during these stores. Without cooling the beam sizes reach the dynamic aperture limit by the time the injection in the blue ring is finished and stay almost unchanged through the store. The beam sizes get substantially reduced during the cooled store.

Figure 8 shows the rate of events registered by the STAR detector for the same stores.

The positive effect of the good cooling on the event rate, illustrated in Fig. 8, is a part of multi-parametric optimization of RHIC operations for the two cases. Among other aspects, this includes the fine-tuning of the RHIC rings working point, the lengthened cooled stores due to a slower decay in the event rate, an ability to perform a beta-squeeze of the cooled stores (in the shown example it is happening at $\approx 900 \text{ s}$ into the cooled store), and a reduced STAR background due to the longitudinal cooling eliminating the ion debunching.

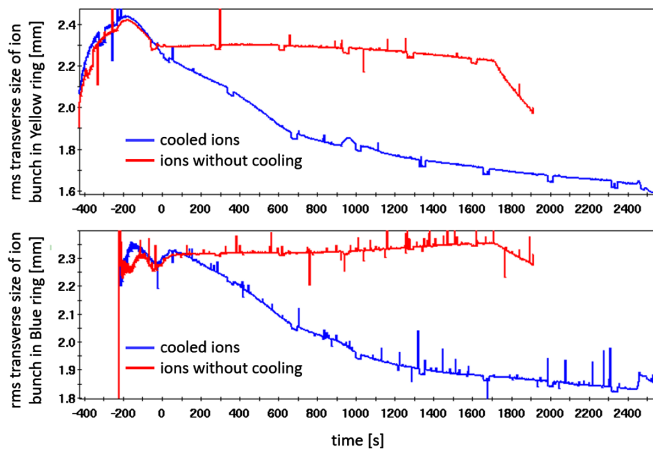


FIG. 7. Transverse beam size of ion bunches in the yellow (top) and the blue (bottom) RHIC rings for cooled (blue line) and not cooled (red line) stores. The spikes and the periodic (5 min) abrupt steps in the signal are artifacts of the measurement system.

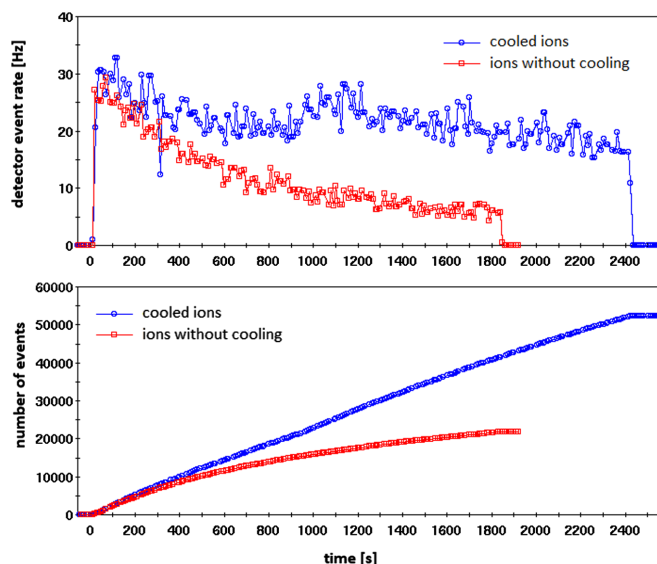


FIG. 8. Event rate (top plot) and number of accumulated events registered by RHIC detector (bottom plot) for cooled (blue line) and not cooled (red line) stores.

The ion and electron beam parameters corresponding to Fig. 7 and 8 are given in Table I.

Data shown in Fig. 7 provide the measurement of the transverse cooling rate.

For example, the transverse beam size of the ions in the yellow CS got reduced from 2.24 mm to 2.1 mm in the first five minutes after the injection cycle was finished and the collisions were established. The corresponding average emittance of the ion bunch was about 0.3 mm · mrad, its intensity was 7.5×10^8 ions per bunch and the rms bunch length was 9.5 ns. The IBS-driven rate of size growth for such a bunch is 0.052 min^{-1} . Then, the measured cooling rate is 0.065 min^{-1} .

TABLE I. Ion and electron beam parameters.

Parameter	Value
γ -factor	4.9
CS length [m]	20
RHIC circumference [m]	3834
<i>ion beam</i>	
Initial bunch intensity	10^9
Initial bunch geometric emittance [mm · mrad]	0.3
Bunch β function in CS [m]	20
Initial bunch rms length [ns]	10.5
<i>electron beam</i>	
Bunch charge [pC]	65
Number of bunches per macro-bunch	30
Average beam current [mA]	18
Bunch geometric emittance [mm · mrad]	0.3
Bunch β function at CS entrance [m]	30
Bunch full length [ps]	350

The ion bunch is cooled by a macrobunch of thirty electron bunches with 65 pC/bunch charge. The transverse cooling rate for an individual ion in the laboratory frame is given by:

$$\lambda_t = \frac{F_t \eta}{\gamma m_i v_i} \quad (17)$$

where F_t is the transverse component of the friction force given by Eq. (1), η is the duty factor taking into account both the ratio of the CS length to the RHIC ring circumference and the probability of ion electron interaction over the period of one synchrotron oscillation, m_i is the ion mass and v_i is the ion velocity. Integrating Eq. (17) over the ion velocity distribution and averaging it over the betatron phases, taking into account the transverse distribution of the electron bunch in the cooling section, we get the

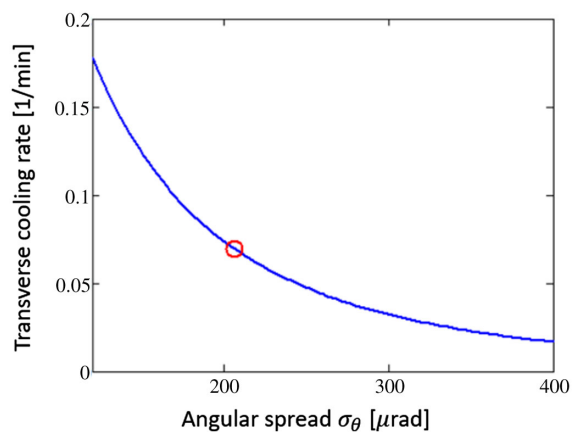


FIG. 9. The rms cooling rate depending on the average angular spread of the electron bunch. The circle represents the experimentally achieved cooling rate.

dependence of the rms cooling rate on the average ion-electron angles (see Fig. 9).

The measured cooling rate corresponds to the rms ion-electron angles of $214 \mu\text{rad}$. The electron bunch angular spread, including both the angles driven by thermal emittance and the angles due to space charge focusing, is about $160 \mu\text{rad}$. Therefore, the correlated ion-electron angles are about $140 \mu\text{rad}$. In this analysis we add the average trajectory angle and the angular spread in quadrature. Such a treatment is justified both because the misaligned trajectory of the electron beam is wiggling through the CS rather than being a straight line and because in the absence of the feedback it is drifting substantially during each ion store. Experimental observations confirmed the validity of this approach for LEReC case.

The excessive ion-electron trajectory angle is caused by fast electron beam motion. Presently, we are working both on pinpointing the source of the beam motion and mitigating it with the trajectory feedback based on the correction algorithm described in Sec. III F.

While further improvements in trajectory alignment and stability are possible, the currently achieved overall electron-ion angles provided the first operational electron cooling of the ion bunches in the collider.

V. CONCLUSION

We discussed our experience with attaining an electron beam with a small angular spread for a nonmagnetized rf-based electron cooler, and with achieving an effective transverse cooling of the colliding ion bunches.

There are numerous factors adversely affecting the electron-ion angles.

The angular spread driven by canonical angular momentum and beam trajectory angles driven by ambient magnetic field, were successfully mitigated by the proper physical design of the cooling section.

Adequate thermal emittance of electron bunch was obtained during commissioning of the electron cooler injector.

The two main challenges in achieving the high transverse cooling rate were the space charge focusing of electron bunches by the ions and obtaining an accurate alignment of electron and ion trajectories.

The ion-electron focusing was partially mitigated by careful tuning of the cooler parameters guided by numerical simulations of this effect. Further improvements in reducing ion-electron focusing are expected from implementing electron macrobunches with omitted central bunches and from lengthening the electron bunches. Both of these measures are a subject of the planned LEReC upgrade.

Accurate alignment of the ion and electron trajectories was obtained after implementation of the BPMs channel switching and utilization of the fast automatic trajectory correction. Proper trajectory alignment resulted in a substantial improvement in the transverse cooling rate, which

resulted in an increase of the integrated RHIC luminosity during the 2020 physics run.

ACKNOWLEDGMENTS

The reported results could not be achieved without dedicated efforts of the entire staff of the BNL Collider-Accelerator Department. This work was supported by the U.S. Department of Energy under contract No. DE-SC0012704.

-
- [1] G. I. Budker, An effective method of damping particle oscillations in proton and antiproton storage rings, *At. Energy*. **22**, 346 (1967) [*Sov. At. Energy* **22**, 438 (1967)].
 - [2] S. van der Meer, Stochastic cooling and the accumulation of antiprotons, *Rev. Mod. Phys.* **57**, 689 (1985).
 - [3] M. Blaskiewicz, J. M. Brennan, and F. Severino, Operational Stochastic Cooling in the Relativistic Heavy-Ion Collider, *Phys. Rev. Lett.* **100**, 174802 (2008).
 - [4] A. Fedotov *et al.*, Experimental Demonstration of Hadron Beam Cooling Using Radio-Frequency Accelerated Electron Bunches, *Phys. Rev. Lett.* **124**, 084801 (2020).
 - [5] S. Chandrasekhar, Brownian motion, dynamical friction and stellar dynamics, *Rev. Mod. Phys.* **21**, 383 (1949).
 - [6] G. I. Budker *et al.*, Experimental study of electron cooling, *Part. Accel.* **7**, 197 (1976), <http://cds.cern.ch/record/1021068/files/p197.pdf>.
 - [7] H. Poth, Applications of electron cooling in atomic, nuclear and high-energy physics, *Nature (London)* **345**, 399 (1990).
 - [8] S. Nagaitsev *et al.*, Experimental Demonstration of Relativistic Electron Cooling, *Phys. Rev. Lett.* **96**, 044801 (2006).
 - [9] S. Seletskiy, Ph.D. thesis, University of Rochester, 2005.
 - [10] A. Shemyakin *et al.*, Attainment of an MeV-range, DC electron beam for the Fermilab cooler, *Nucl. Instrum. Methods Phys. Res., Sect. A* **532**, 403 (2004).
 - [11] A. Burov, S. Nagaitsev, A. Shemyakin, and Y. Derbenev, Optical principles of beam transport for relativistic electron cooling, *Phys. Rev. Accel. Beams* **3**, 094002 (2000).
 - [12] L. Mao *et al.*, Experimental demonstration of electron cooling with bunched electron beam, in *Proc. of Workshop on Beam Cooling and Related Topics (COOL17)*, Bonn, Germany, 18-22 September (JACoW Publishing, Geneva, 2017).
 - [13] Y. Zhang, Experimental demonstration of ion beam cooling with pulsed electron beam in *Proc. 9th International Particle Accelerator Conference (IPAC18)*, Vancouver, BC, Canada, April 29-May 4 (JACoW, Geneva, 2018).
 - [14] A. Fedotov, I. Ben-Zvi, D. L. Bruhwiler, V. N. Litvinenko, and A. O. Sidorin, High-energy electron cooling in a collider, *New J. Phys.* **8**, 283 (2006).
 - [15] Electron Ion Collider Pre-Conceptual Design Report, BNL Report No. BNL-211943-2019-FORE, 2019.
 - [16] X. Gu *et al.*, Stable operation of a high-voltage high-current dc photoemission gun for the bunched beam electron cooler in RHIC, *Phys. Rev. Accel. Beams* **23**, 013401 (2020).

- [17] B. Xiao *et al.*, Design and test of 704 MHz and 2.1 GHz normal conducting cavities for low energy RHIC electron cooler, *Phys. Rev. Accel. Beams* **22**, 030101 (2019).
- [18] S. Seletskiy *et al.*, Accurate setting of electron energy for demonstration of first hadron beam cooling with rf-accelerated electron bunches, *Phys. Rev. Accel. Beams* **22**, 111004 (2019).
- [19] D. Kayran *et al.*, High-brightness electron beams for linac-based bunched beam electron cooling, *Phys. Rev. Accel. Beams* **23**, 021003 (2020).
- [20] H. Zhao *et al.*, Cooling simulations and experimental benchmarkign for an rf-based electron cooler, *Phys. Rev. Accel. Beams* **23**, 074201 (2020).
- [21] S. Chandrasekhar, *Principles of Stellar Dynamics* (University of Chicago Press, Chicago, 1942).
- [22] Y. S. Derbenev and A. N. Skrinsky, The effect of an accompanying magnetic field on electron cooling, *Part. Accel.* **8**, 235 (1978), <https://cds.cern.ch/record/1107957/files/p235.pdf>.
- [23] J. Kewisch, A. V. Fedotov, D. Kayran, and S. Seletskiy, Beam optics for the RHIC low energy electron cooler (LReC), in *Proceedings of NAPAC16, Chicago, IL* (JACoW Publishing, Geneva, 2016).
- [24] S. Seletskiy, A. Fedotov, and D. Kayran, Beam dynamics in non-magnetized electron cooler with strong hadron-electron focusing, BNL Report No. BNL-216225-2020-TECH, 2020.
- [25] R. D. Ruth, A canonical integration technique, *IEEE Trans. Nucl. Sci.* **30**, 2669 (1983).
- [26] S. Seletskiy, M. Blaskiewicz, A. Fedotov, D. Kayran, and J. Kewisch, Effect of beam-beam kick on electron beam quality in first bunched electron cooler, *J. Phys. Conf. Ser.* **1350**, 012134 (2019).
- [27] S. Seletskiy *et al.*, Physical design of magnetic shielding for LReC cooling section, BNL Report No. BNL-112084-2016-IR, 2016.
- [28] S. Seletskiy *et al.*, Finalized configuration of magnetic shielding for LReC cooling section, BNL Report No. BNL-114736-2017-IR, 2017.
- [29] S. Seletskiy *et al.*, Alignment of electron and ion beam trajectories in nonmagnetized electron cooler, in *Proceedings of IPAC17, Copenhagen, Denmark* (JACoW Publishing, Geneva, 2017).
- [30] Z. Sorrell, P. Cerniglia, R. Hulsart, K. Mernick, and R. Michnoff, Beam position monitors for LReC, BNL Report No. BNL-112674-2016-CP, 2016.
- [31] R. Hulsart, R. Michnoff, P. Thieberger, and S. Seletskiy, Some considerations about switching BPM channels, BNL Report No. BNL-213694-2020-TECH, 2020.
- [32] K. A. Brown, M. Harvey, Y. Jing, P. Kankiya, and S. Seletskiy, Online simulation framework through HTTP services, in *Proceedings of ICALEPCS2017, Barcelona, Spain* (JACoW Publishing, Geneva, 2017).
- [33] M. Blaskiewicz and J. Kewisch, Emittance growth generated by bunched beam electron cooling, BNL Report No. BNL-211519-2019-TECH, 2019.